NACA RM E58D04a

RESEARCH MEMORANDUM

EXPERIMENTAL PERFORMANCE OF A 0.35 HUB-TIP RADIUS RATIO TRANSONIC AXIAL-FLOW-COMPRESSOR STAGE DESIGNED FOR 40 POUNDS PER SECOND PER UNIT FRONTAL AREA

By Richard R. Cullom, John C. Montgomery, and Paul T. Yasaki

Lewis Flight Propulsion Laboratory
Cleveland, Ohio

NATIONAL ADVISORY COMMITTEE
FOR AERONAUTICS

WASHINGTON

September 4, 1958

NATIONAL ADVISORY COMMITTEE FOR AERONAUTICS

RESEARCH MEMORANDUM

EXPERIMENTAL PERFORMANCE OF A 0.35 HUB-TIP RADIUS RATIO TRANSONIC AXIAL-FLOW-COMPRESSOR STAGE DESIGNED FOR 40 POUNDS PER SECOND PER UNIT FRONTAL AREA*

By Richard R. Cullom, John C. Montgomery
and Paul T. Yasaki

SUMMARY

An investigation was conducted to determine the over-all stage and stator blade-element performance of a transonic axial-flow-compressor inlet stage. A transonic inlet stage with a hub-tip radius ratio of 0.35 was designed to produce a total-pressure ratio of 1.49 with a tip relative inlet Mach number of 1.27 and an equivalent specific weight flow of 40 pounds per second per square foot of frontal area. The stator blade-element performance is presented herein for a blade row with a design absolute inlet hub Mach number of 0.99. The rotor design and over-all performance were reported previously.

At design equivalent tip speed of 1100 feet per second, the stage attained an equivalent weight flow of 37.6 pounds per second per square foot of frontal area at a total-pressure ratio of 1.42 and an adiabatic efficiency of 0.84. Peak adiabatic stage efficiencies of 0.93, 0.92, 0.89, and 0.84 were obtained at 60, 80, 90, and 100 percent of design speed, respectively.

The installation of stator blades did not appreciably detract from the flow range of the rotor alone. A significant decrease in efficiency was noted as the major performance penalty incurred by the addition of stators. The high total-pressure-loss coefficient experienced at the stator hub section was attributed to the acceleration of the high subsonic relative inlet Mach number to a supersonic value on the highly cambered anterior region of the suction surface. A strong shock system was produced that accounted for the excessive losses.

---

*Title, Confidential.

INTRODUCTION

Turbojet engines with high ratios of thrust to engine weight are essential for aircraft propulsion at high flight speeds. One method of increasing the engine thrust per unit engine weight is to increase the weight flow per unit frontal area through the engine. This can be accomplished by using a transonic inlet stage in a multistage axial-flow compressor. Transonic axial-flow-compressor stages are capable of producing high pressure ratio and high weight flow per unit frontal area at relatively high efficiencies (refs. 1 and 2). The weight flow per unit frontal area can be increased over that of previous transonic stage designs by decreasing the hub-tip diameter ratio and by increasing the inlet axial Mach number. However, high-weight-flow designs are often associated with a stator blade design problem, in that for a given stage work output the stator hub inlet Mach number increases as the hub-tip diameter ratio is decreased and the inlet axial Mach number is increased.

The transonic axial-flow-compressor inlet stage used in this investigation (ref. 3) was designed to determine the feasibility of increasing the weight flow per unit frontal area by reducing the hub-tip diameter ratio to 0.35 and by increasing the absolute average inlet Mach number to 0.76. The blade-element and over-all performance of the rotor alone is presented in reference 3. The blade-element performance of the stators and the over-all stage performance based on detailed instrument surveys are presented herein for 60, 80, 90, and 100 percent of design corrected rotor tip speed.

SYMBOLS

A_F compressor frontal area, sq ft

c blade chord, in.

D diffusion factor

i incidence angle, angle between inlet-air direction and tangent to blade mean camber line at leading edge, deg

M Mach number

P total pressure, lb/sq ft

r radius, in.

t blade thickness, in.

U blade speed, ft/sec

V velocity of air, ft/sec

w integrated weight flow at rotor inlet, lb/sec

β air angle, angle between air velocity vector and axial direction, deg

δ ratio of inlet total pressure to NACA standard sea-level pressure of 2116.2 lb/sq ft

δ° deviation angle, angle between outlet-air direction and tangent to blade mean camber line at trailing edge, deg

η adiabatic efficiency

θ ratio of inlet total temperature to NACA standard sea-level temperature of 518.7° R

σ solidity, ratio of blade chord to blade spacing

φ blade camber angle, difference between angles of tangents to mean camber line at leading and trailing edges, deg

$\bar{\omega}$ total-pressure-loss coefficient

Subscripts:

min minimum loss

R rotor

S stator

z axial direction

0 compressor depression tank

1 rotor inlet

2 rotor outlet or stator inlet

3 stator outlet

Superscript:

' relative

APPARATUS AND PROCEDURE

Rotor Design

The rotor design is presented in detail in reference 3. The rotor employed double-circular-arc blade profile sections and was designed for constant radial energy addition. Radial-equilibrium conditions that neglect the entropy term in the equations of motion were assumed for velocity-distribution calculations. The rotor was designed to produce a pressure ratio of 1.51 at an equivalent weight flow of 40 pounds per second per square foot of frontal area and a tip speed of 1100 feet per second at an adiabatic efficiency of 0.95. The inlet diameter of the rotor was 14 inches, and the hub-tip diameter ratio was 0.35. The design inlet relative Mach number varied from 0.74 at the hub to 1.27 at the tip. The rotor blade design values and geometry are summarized in table I.

Stator Design

The stators were designed for axial discharge so that high relative inlet Mach numbers could be obtained for succeeding stage designs. The design stator axial velocity ratio was to have an average value of unity. The stators were designed to produce a stage total-pressure ratio of 1.49 at an equivalent weight flow of 40 pounds per second per square foot of frontal area. The stator design inlet conditions were the rotor design outlet conditions. The stator design inlet-air angle (measured from the axial direction) varied from 23° at the tip to 46.2° at the hub. The design absolute inlet Mach number varied from 0.87 at the tip to 0.99 at the hub.

A double-circular-arc blade profile with a constant chord of 2 inches and a constant thickness-to-chord ratio of 0.06 was designed. Because of an error in fabrication, the actual thickness-to-chord ratio was 0.03. The stator discharge area was increased 1 percent over the theoretical discharge area to allow for the assumed growth of the wall boundary layer. A summary of the stator blade design values and geometry is given in table II.

Compressor Installation

The compressor installation (fig. 1) is the same as that described in reference 3, except that stator blades were added to obtain the stator blade-element and over-all stage performance. In addition, the rotor discharge passage area, which was increased in reference 3 to prevent choking for tests of the rotor alone, was changed to the design condition of constant tip diameter for the rotor-stator combination as shown in figure 1.

Instrumentation

The axial measuring stations used to observe the stage performance conditions are shown in figure 1. Stations 1 ($\frac{1}{2}$ in. upstream of the rotor blade hub leading edge) and 2 ($\frac{1}{2}$ in. downstream of the rotor blade hub trailing edge) were used to observe the rotor inlet and outlet conditions, respectively. These stations were at the same axial locations as those used to obtain the rotor performance in reference 3. Station 3 (1 in. downstream of the stator blade hub trailing edge) was used to observe the stator outlet conditions.

At the rotor inlet (station 1), total pressure and air angle were measured at all radial survey stations: 3, 5, 7, 10, 30, 50, 70, 90, 93, 95, and 97 percent of the blade passage height from the outer wall. The static pressure was measured at the walls and at the five major radial stations (10, 30, 50, 70, and 90 percent of the blade passage height from the outer wall). At the rotor outlet (station 2), total temperature, total pressure, and air angle were measured at all radial survey stations. Static pressure was measured at the five major radial stations and at the walls.

Downstream of the stators (station 3), total temperature, total pressure, and air angle were measured and recorded continually by an automatic recorder as each instrument was traversed circumferentially across one blade passage. Circumferential surveys were made at the five major radial stations. Static pressure was constant circumferentially across the stator exit passage and was therefore measured along a midpassage radial line at the five major stations. Static pressure was also observed at the walls.

Procedure

The stator blade-element performance and the over-all stage performance were obtained in this phase of the investigation. The stator and complete stage data were taken with an inlet pressure of 20 inches of mercury absolute at 60, 80, 90, and 100 percent of rotor design speed. The performance data were obtained from radial surveys at a given axial station. The stator outlet performance was obtained by averaging the circumferential survey data.

Computations

The computational procedure was, in general, similar to that of reference 3. The air and blade angles used in the equations are illustrated in figure 2.

The integrated weight flows measured at the three axial stations agreed within 5 percent with the values measured by the thin-plate orifice, 80 percent of these measurements being within 3 percent of the orifice weight flow. The integrated mass-averaged adiabatic efficiencies agreed within approximately 5 percent with the integrated mass-averaged momentum efficiencies. Over half the mass-averaged adiabatic and momentum efficiencies agreed within 3 percent.

RESULTS AND DISCUSSION

Over-All Performance

The mass-averaged over-all stage performance is presented in figure 3 as the total-pressure ratio and adiabatic efficiency plotted against equivalent specific weight flow based on weight-flow measurements at station 1 for equivalent tip speeds of 60, 80, 90, and 100 percent of design. At design speed the maximum equivalent weight flow of 38.2 pounds per second per square foot of frontal area was obtained. The maximum stage total-pressure ratio obtained at design speed was 1.44 at a weight flow of 36.8 pounds per second per square foot of frontal area at an adiabatic efficiency of 0.82. Peak adiabatic stage efficiencies of 0.93, 0.92, 0.89, and 0.84 were obtained at 60, 80, 90, and 100 percent of design speed, respectively. At design speed and maximum efficiency the stage attained an equivalent weight flow of 37.6 pounds per second per square foot of frontal area at a pressure ratio of 1.42.

The over-all performance of the rotor with and without stator blades is presented in figure 4 to illustrate the performance loss attributed to the presence of stator blades. The total-pressure ratio and efficiency obtained at stations 2 and 3 for the rotor alone and for the stage, respectively, are presented as a function of the equivalent weight flow. The maximum weight flow at design speed for the rotor alone was 38.70 pounds per second per square foot of frontal area. At design speed a maximum total-pressure ratio of 1.53 was obtained for the rotor alone at a weight flow of 36.70 pounds per second per square foot of frontal area. The maximum rotor efficiencies were 0.98, 0.96, 0.93, and 0.89 at 60, 80, 90, and 100 percent of design speed, respectively.

The installation of stator blades did not appreciably detract from the flow range of the rotor alone. A significant decrease in efficiency was noted as the major performance penalty incurred by the addition of stators.

The rotor inlet or stage inlet conditions are presented in reference 3 as radial variations of the relative inlet-air angle, relative inlet Mach number, and axial inlet Mach number at 60, 80, and 100 percent of design speed. The radial variations of the design inlet conditions are

also presented. The design inlet conditions were not attained, because the design weight flow was not realized. The weight-flow deficiency was due to improper choice of optimum rotor incidence angle (ref. 3). The predicted radial distribution was correct, but because of the weight-flow deficiency the desired magnitude of the inlet conditions was not achieved. The radial variations of the relative inlet-air angle, relative inlet Mach number, and axial inlet Mach number at 80 and 60 percent of design speed (ref. 3) were similar to those of the respective parameters at design speed.

The stage performance at 80-percent design speed appeared highly suitable for a transonic inlet stage on present engines. A stage total-pressure ratio of 1.28 at a weight flow of 34.6 pounds per second per square foot of frontal area was attained at an adiabatic efficiency of 0.92.

Stator Blade-Element Performance

In order to gain better insight into the internal flow mechanisms and to facilitate the evaluation of the losses in the stator blades, detailed blade-element data are presented. To further evaluate the losses, supplementary data in the form of stator blade wake profiles and the variation of minimum-loss level with stator inlet Mach number are included. The stator inlet and outlet conditions are presented for comparison with their respective design variation.

Inlet conditions. - The rotor outlet or stator inlet conditions from reference 3 are presented in figure 5. The rotor absolute outlet-air angle and the rotor absolute outlet Mach number correspond to the stator absolute inlet-air angle and the stator absolute inlet Mach number, respectively. The stator absolute inlet-air angle and absolute inlet Mach number are presented as functions of radius at three weight-flow points for 60, 80, and 100 percent of design speed.

The design stator absolute inlet-air angle (fig. 5(a)) was not attained at all radial sections. At the peak-efficiency weight flow, it was approximately 5° higher at the tip section and 4.5° lower at the hub section than the design values. This discrepancy was due to the fact that the stator geometry was established by the design rotor discharge conditions, which were not realized. The absolute stator inlet Mach number (fig. 5(b)) at maximum-efficiency weight flow and design speed varied from approximately 0.83 near the tip to 0.93 at the hub section.

The absolute inlet-air angle and Mach number did not correlate well with the design values. The discrepancy can be attributed primarily to deleting the entropy term in the equation of motion used in the design calculations and the failure to predict the optimum rotor incidence angle.

The absolute inlet-air angle and Mach number at other speeds and weight flows had similar radial variation for their respective parameters.

Blade-element characteristics. - The stator blade-element characteristics are presented in figure 6 at four tip speeds for the five major radial stations. The diffusion factor, axial velocity ratio, absolute inlet Mach number, deviation angle, and total-pressure-loss coefficient are presented as functions of the incidence angle.

At minimum-loss incidence angle the stator deviation angles at all sections were within 1.5° of the design deviation angles given in table II. The minimum-loss deviation angles were within 2° of Carter's rule at all radial positions.

The variation of total-pressure-loss coefficient shows a tendency for the low-loss incidence-angle range to decrease as the inlet Mach number is increased.

The radial variation of stator diffusion factor is shown in figure 7. The diffusion factor at maximum-efficiency weight flow agrees very well with the design values except at the hub, where the decrease in velocity ratio causes the diffusion factor to increase above the design value.

Evaluation of total-pressure loss. - The variation of minimum stator total-pressure-loss coefficient with stator inlet Mach number is shown in figure 8 for three radial positions. All radial sections of the stator blade operated at a fairly constant value of minimum-loss coefficient of approximately 0.035 for inlet Mach numbers below 0.78.

The magnitude of the minimum total-pressure-loss coefficient at the stator hub increased sharply with increased inlet Mach number above 0.78. At design speed the minimum loss at the hub section (radial position E) was 0.159, which was approximately three times the minimum loss at the other sections. The increased loss at the stator hub section can be explained by the supposition of the following flow model. The magnitude of the stator hub inlet Mach number measured $\frac{1}{2}$ inch upstream of the stator blade hub leading edge was in the high subsonic range at design rotor tip speed. The streamlines at the stator blade leading edge converged because of the presence of the blade to produce an exterior throat. The slight area contraction thus produced raised the high subsonic inlet velocity to free-stream sonic velocity. The flow was further accelerated over the highly cambered anterior portion of the suction surface by means of supersonic turning, and the high Mach numbers in that region produced strong shock-wave systems and associated high losses.

The occurrence of supersonic channel flow in blade rows with subsonic inlet conditions is substantiated by the cascade studies of references 4 and 5. The supersonic flow is sharply decelerated by the shock system, and the suction-surface boundary layer is subject to a large static-pressure rise. The peak suction-surface Mach numbers computed by the Prandtl-Meyer method were 1.5 or greater at the hub section, and therefore separation of the boundary layer is probable (ref. 6). Figure 9 shows the circumferential variation of the stator outlet total pressure at three radial positions. The relatively large wake pressure defect at the hub section may indicate suction-surface boundary-layer separation in addition to depicting the shock losses.

A combination of the high subsonic inlet hub Mach number and the stator blade geometry produced the flow conditions required to use the shock-loss analysis of reference 7. The loss calculation of reference 7 and the Prandtl-Meyer method both require a sonic inlet velocity. Because of the high subsonic inlet Mach number and the exterior throat at the hub section, it was theorized that sonic inlet conditions did exist, so that these methods could be used to analyze the stator losses quantitatively. If the loss coefficient attributed to the passage shock loss as computed by the method of reference 7 is added to the profile loss obtained from typical cascade and stator data of reference 8, this predicted total loss compares favorably with the value experimentally obtained. From these computations, it was observed that the passage shock loss accounted for approximately half the total loss.

This trend in stator hub total-pressure-loss coefficient with absolute inlet Mach number is similar to the loss variation observed at the tip region of a number of rotors (ref. 8). The Mach number at which the rotor tip-section loss coefficients increased rapidly was above that indicated for the stator hub section, because the camber of rotor tip sections was usually lower than that of stator hub sections.

The minimum total-pressure-loss coefficient at the mean radial blade section (fig. 8) did not increase very rapidly with inlet Mach number because of the lower curvature of the anterior portion of the suction surface. In addition, for a given stator inlet Mach number, the mean section operated at a lower value of incidence angle than the hub section. The lower curvature and incidence angle decreased the total amount of supersonic turning and therefore limited the value of the blade surface Mach number. Therefore, at a given inlet Mach number, the maximum blade surface velocity at the mean section was lower than that at the hub. The passage shock at the mean section then occurred at a lower Mach number, and the shock loss was decreased. In addition, the lower surface velocity reduced the severity of the flow separation and thus further reduced the loss.

[redacted]

The total-pressure-loss coefficient at the tip radial blade section appears to be relatively unaffected by inlet Mach number variation (fig. 8). This trend in loss coefficient can be attributed to the lower cambered section, which does not appreciably accelerate the flow over the suction surface.

The minimum-loss incidence angle was higher than the design incidence angle at all blade sections except the hub (fig. 10). The design rule of reference 9 was obtained from rotor blade-element data. By use of the blade-element concept, this rule was applied to the stator design. The blade-element concept does not consider three-dimensional effects, which possibly are different for rotating and stationary blade rows. Therefore, the difference between the experimental and design values can be attributed to three-dimensional effects.

The radial variation of incidence angle at maximum-efficiency weight flow is also shown in figure 10. The maximum-efficiency incidence angle was approximately 5° higher at the tip and 4.3° lower at the hub section than the respective design values. As stated previously, this off-design operation resulted from using the design distribution of rotor outlet-air angle, which was not attained, to establish the stator blade geometry. At peak-efficiency weight flow, the actual absolute inlet-air angle was approximately 5° higher than the design value in the tip region and 4.5° lower than design inlet angle at the hub. Since the loss coefficient remained relatively constant over a large range of incidence angles in the stator tip region, the tip blade sections still operated at a low-loss value even at the off-design incidence angles.

It should be noted that the comparison made in figure 10 is not a valid test of the design rule of reference 9. The design values of inlet absolute Mach number and inlet absolute air angle were used to compute the design incidence angle. In this investigation the design values of inlet absolute Mach number and inlet absolute air angle were not experimentally attained; therefore, the angle discrepancy cannot be attributed to design-rule inaccuracies alone.

Outlet conditions. - The radial variations of the stator absolute outlet Mach number, absolute outlet-air angle, axial velocity ratio, and total-pressure-loss coefficient are plotted in figure 11. The data are presented for three equivalent weight flows at 60, 80, and 100 percent of design tip speed.

The absolute outlet Mach number did not correlate with the design radial variation. The sharp drop in outlet Mach number in the hub region at design speed can be attributed to the high losses caused by the shock system in that portion of the passage. The outlet Mach number drop in the hub region was progressively less pronounced as the tip speed decreased.

The axial velocity ratio at maximum-efficiency weight flow closely approximates the design distribution except at the hub section. In this region the high losses attributed to the shock system sharply decreased the outlet velocity.

The total-pressure-loss coefficient at design speed increased sharply at the hub section because of the previously discussed shock phenomenon. The rise in loss coefficient at the stator tip may be attributed to operation of the blade section in a region of low-energy flow. At 80 percent of design speed and maximum efficiency, the midstream section of the stator operated at a very low loss level.

The stator absolute outlet-air angle at design speed and maximum-efficiency weight flow was within approximately 3° of the design axial discharge angle. As the speed decreased, the stator outlet-air angle approached the desired axial direction. At 80 percent of design speed the discharge angle at maximum efficiency was within 1.5° of axial discharge.

Summary Remarks

The stage performance at design speed was penalized by the relatively high losses encountered in the stator, especially in the hub region. By the study of a flow model, a quantitative loss analysis was conducted. The source of the stator losses was the supersonic blade surface Mach numbers, which produced passage shock systems and flow separation. A transonic stage design incorporating low stator inlet Mach numbers and low blade camber would probably reduce the losses encountered.

For a given stage weight flow and work input, lower stator Mach numbers can be obtained by increasing the rotor tip speed. When the rotor tip speed increases, for a given work input, the rotor camber and usually the stator camber can be reduced. The rotor tip would normally be operating at a higher loss level because of the increased inlet Mach number, but the decreased camber limits the blade surface velocity and tends to offset the effect of increased inlet velocity. The stator losses would be reduced by the decreased inlet Mach number and the lower blade camber. Therefore, in the flow and pressure-ratio range investigated, transonic stages of high-tip-speed, low-camber design would be preferred if efficiency were of primary importance.

SUMMARY OF RESULTS

Investigation of the over-all and stator blade-element performance of a 0.35 hub-tip radius ratio transonic axial-flow-compressor inlet stage yielded the following results:

1. At rotor design tip speed of 1100 feet per second a maximum stage-total-pressure ratio of 1.44 was obtained at a weight flow of 36.8 pounds per second per square foot of frontal area at an adiabatic efficiency of 0.82. Peak adiabatic stage efficiencies of 0.93, 0.92, 0.89, and 0.84 were obtained at 60, 80, 90, and 100 percent of design speed, respectively.

2. The stage performance at 80-percent design speed appeared highly suitable for a transonic inlet stage on present engines. A stage total-pressure ratio of 1.28 at a weight flow of 34.6 pounds per second per square foot of frontal area was attained at an adiabatic efficiency of 0.92.

3. The installation of stator blades did not appreciably detract from the flow range of the rotor alone. A significant decrease in efficiency was noted as the major performance penalty incurred by the addition of stators.

4. Design procedures that neglect the entropy term in the equations of motion are not sufficiently accurate for the determination of velocity distributions and flow angles in the design of transonic axial-flow-compressor stages with low hub-tip diameter ratios and high pressure ratios.

5. The high total-pressure-loss coefficient encountered at the stator hub section was attributed to the acceleration of the flow over the highly cambered anterior portion of the suction surface to a supersonic Mach number of such magnitude as to produce a strong shock wave. The loss coefficient attributed to the shock system accounted for approximately half the total loss. The passage shock should therefore be of prime concern in designing transonic stators.

6. The stator blade-element deviation angles near minimum-loss incidence angle were within 2° of the values predicted by Carter's rule at all radial positions.

Lewis Flight Propulsion Laboratory
National Advisory Committee for Aeronautics
Cleveland, Ohio, April 10, 1958

[redacted]

REFERENCES

1. Robbins, William H., and Glaser, Frederick W.: Investigation of an Axial-Flow-Compressor Rotor with Circular-Arc Blade Operating up to a Rotor-Inlet Relative Mach Number of 1.22. NACA RM E53D24, 1953.

2. Lieblein, Seymour, Lewis, George W., Jr., and Sandercock, Donald M.: Experimental Investigation of an Axial-Flow Compressor Inlet Stage Operating at Transonic Relative Inlet Mach Numbers. I - Over-All Performance of Stage with Transonic Rotor and Subsonic Stators up to Relative Inlet Mach Number of 1.1. NACA RM E52A24, 1952.

3. Montgomery, John C., and Yasaki, Paul T.: Design and Experimental Performance of a 0.35 Hub-Tip Radius Ratio Transonic Axial-Flow-Compressor Rotor Designed for 40 Pounds per Second per Unit Frontal Area. NACA RM E58D17, 1958.

4. Emery, James C., and Dunavant, James C.: Two-Dimensional Cascade Tests of NACA 65-$(C_{l_o} A_{10})$10 Blade Sections at Typical Compressor Hub Conditions for Speeds up to Choking. NACA RM L57H05, 1957.

5. Dunavant, James C., and Emery, James C.: Two-Dimensional Cascade Investigation at Mach Numbers up to 1.0 of NACA 65-Series Blade Sections at Conditions Typical of Compressor Tips. NACA RM L58A02, 1958.

6. Bogdonoff, Seymour M.: Axial-Flow Compressors. Pt. I - A Study of the Fluid Mechanics Problems Associated with Optimizing Performance. Tech. Rep. TR 54-514, WADC, Oct. 1954. (Contract AF-33(038)-18190.)

7. Schwenk, Francis C., Lewis, George W., and Hartmann, Melvin J.: A Preliminary Analysis of the Magnitude of Shock Losses in Transonic Compressors. NACA RM E57A30, 1957.

8. Lieblein, Seymour, Schwenk, Francis C., and Broderick, Robert L.: Diffusion Factor for Estimating Losses and Limiting Blade Loadings in Axial-Flow-Compressor Blade Elements. NACA RM E53D01, 1953.

9. Robbins, William H., Jackson, Robert J., and Lieblein, Seymour: Blade-Element Flow in Annular Cascades. Ch. VII of Aerodynamic Design of Axial-Flow Compressors. Vol. II. NACA RM E56B03a, 1956.

[redacted]

TABLE I. - ROTOR BLADE DESIGN VALUES AND GEOMETRY

Passage height from tip, percent	Inlet radius, r_1, in.	Outlet radius, r_2, in.	Relative inlet-air angle, β_1', deg	Relative outlet-air angle, β_2', deg	Maximum thickness ratio, t/c	Solidity, σ	Diffusion factor, D	Blade camber angle, φ, deg	Relative inlet Mach number, M_1'	Absolute outlet Mach number, M_2	Incidence angle, i, deg	Deviation angle, δ^o, deg
10	6.59	6.44	52.3	35.5	0.053	0.980	0.347	18.2	1.228	0.858	2.8	4.2
30	5.67	5.75	46.9	29.3	.059	1.118	.385	16.1	1.151	.838	5.6	4.0
50	4.75	5.06	41.8	20.2	.065	1.303	.411	19.0	1.059	.840	7.3	4.6
70	3.83	4.37	37.0	7.3	.071	1.558	.397	27.4	.941	.866	8.4	6.1
90	2.91	3.68	31.9	-9.4	.077	1.938	.303	39.7	.809	.930	9.1	7.5

TABLE II. - STATOR BLADE DESIGN VALUES AND GEOMETRY

Passage height from tip, percent	Inlet radius, r_2, in.	Outlet radius, r_3, in.	Absolute inlet-air angle, β_2, deg	Absolute outlet-air angle, β_3, deg	Maximum thickness ratio, t/c	Solidity, σ	Diffusion factor, D	Blade camber angle, φ, deg	Absolute inlet Mach number, M_2	Absolute outlet Mach number, M_3	Incidence angle, i, deg	Deviation angle, δ^o, deg
10	6.44	6.48	24.75	0	0.060	1.030	0.369	30.7	0.858	0.699	0.50	6.4
30	5.75	5.87	28.60	0	.060	1.150	.353	33.6	.838	.704	2.10	7.1
50	5.06	5.26	33.00	0	.060	1.296	.340	36.9	.840	.717	3.80	7.8
70	4.37	4.64	37.90	0	.060	1.485	.342	40.3	.866	.735	6.30	8.6
90	3.68	4.03	43.30	0	.060	1.737	.357	44.5	.930	.763	8.80	9.9

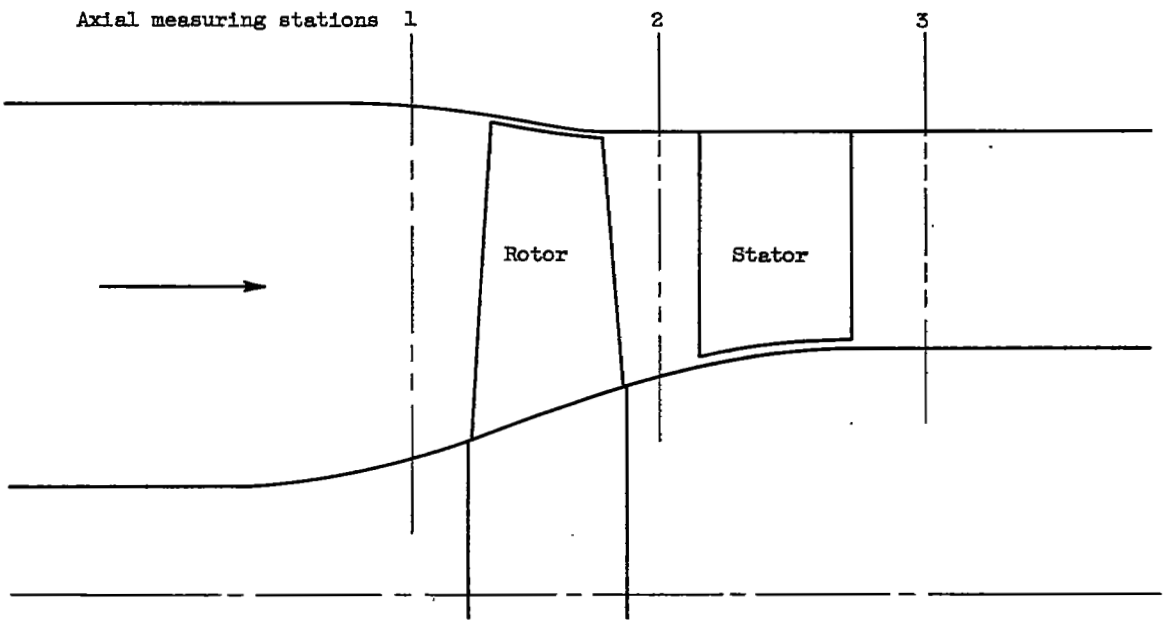

Figure 1. - Schematic diagram of compressor installation.

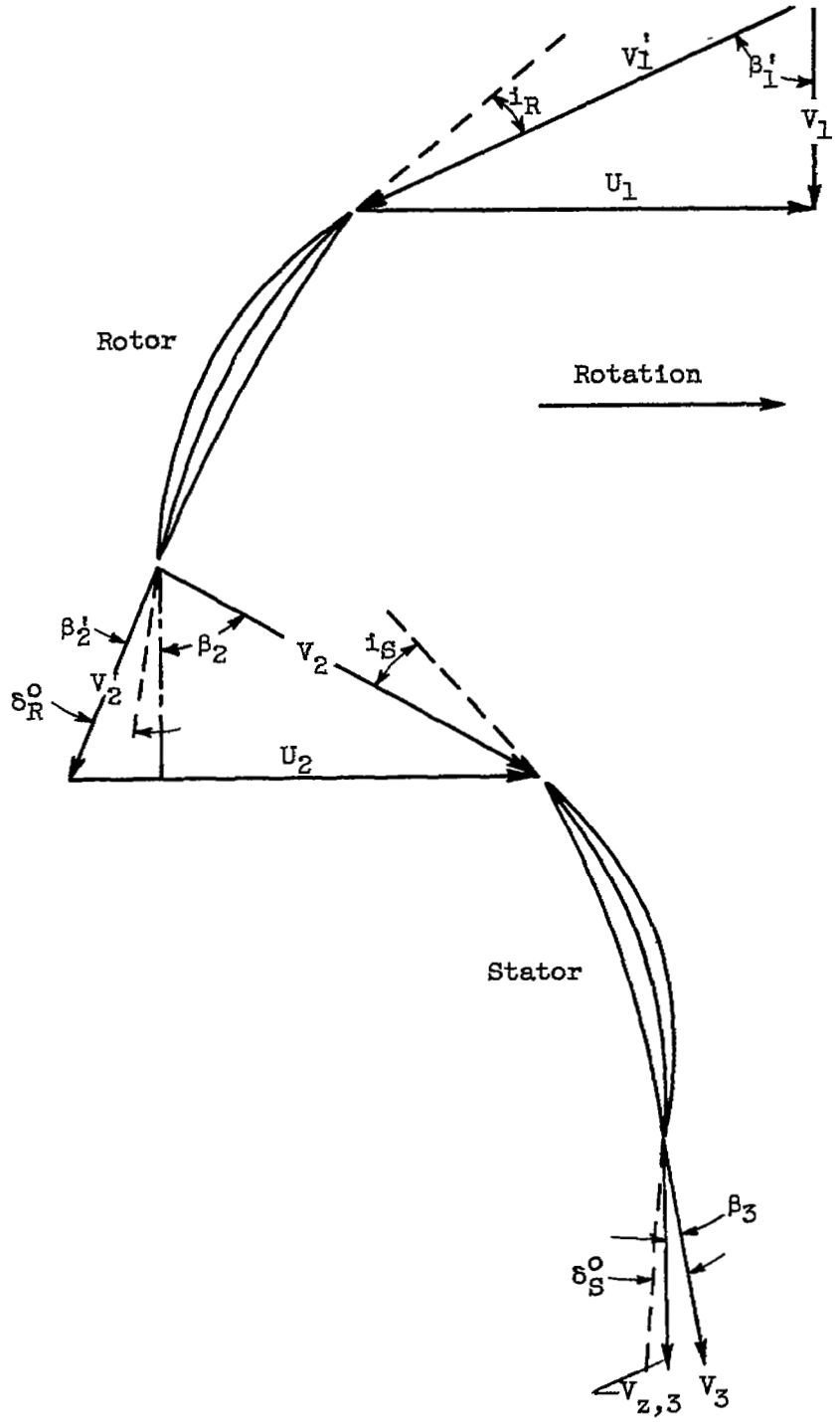

Figure 2. - Air and blade angles for a blade element.

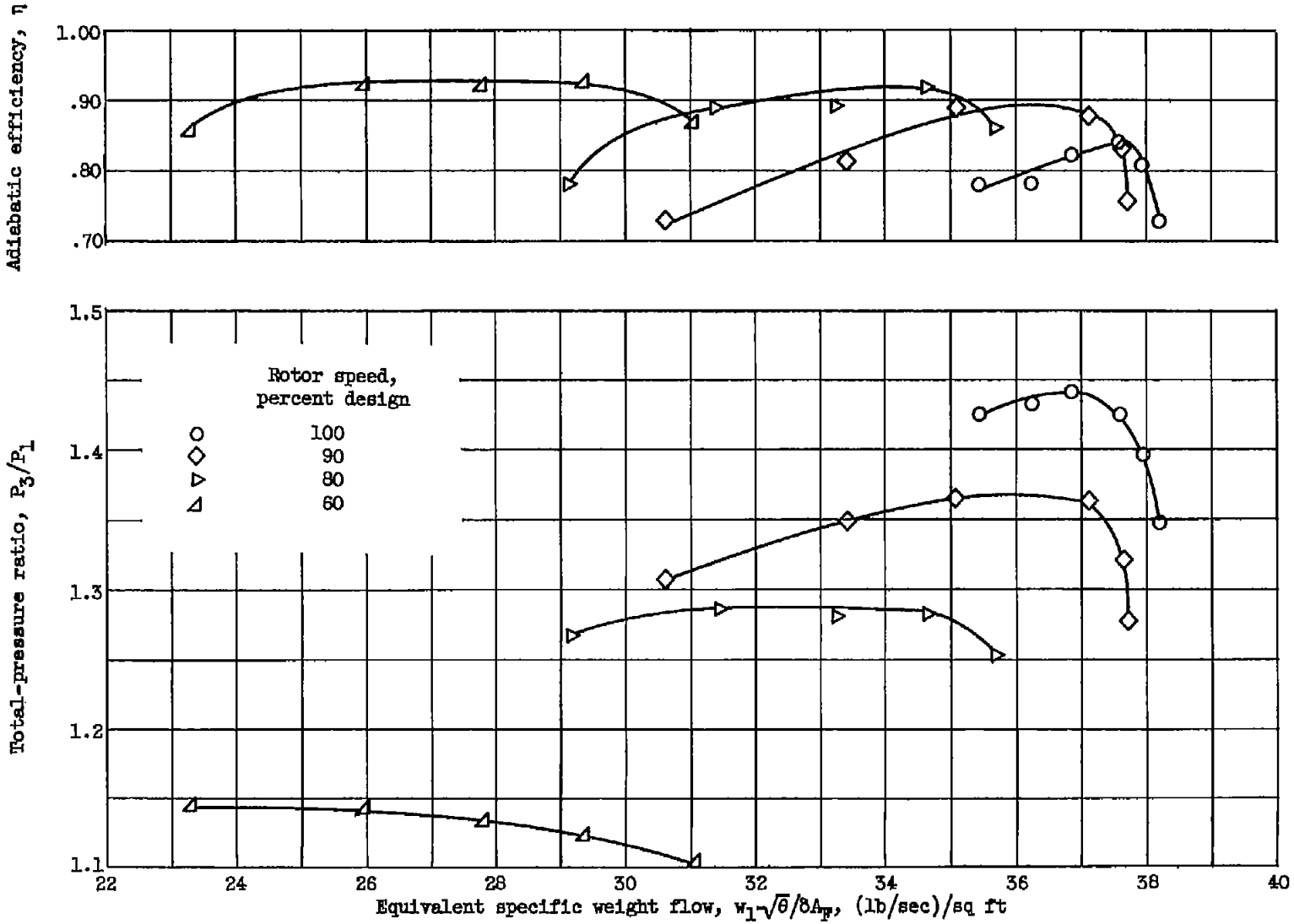

Figure 3. - Mass-averaged over-all performance of 0.35 hub-tip ratio rotor and stator.

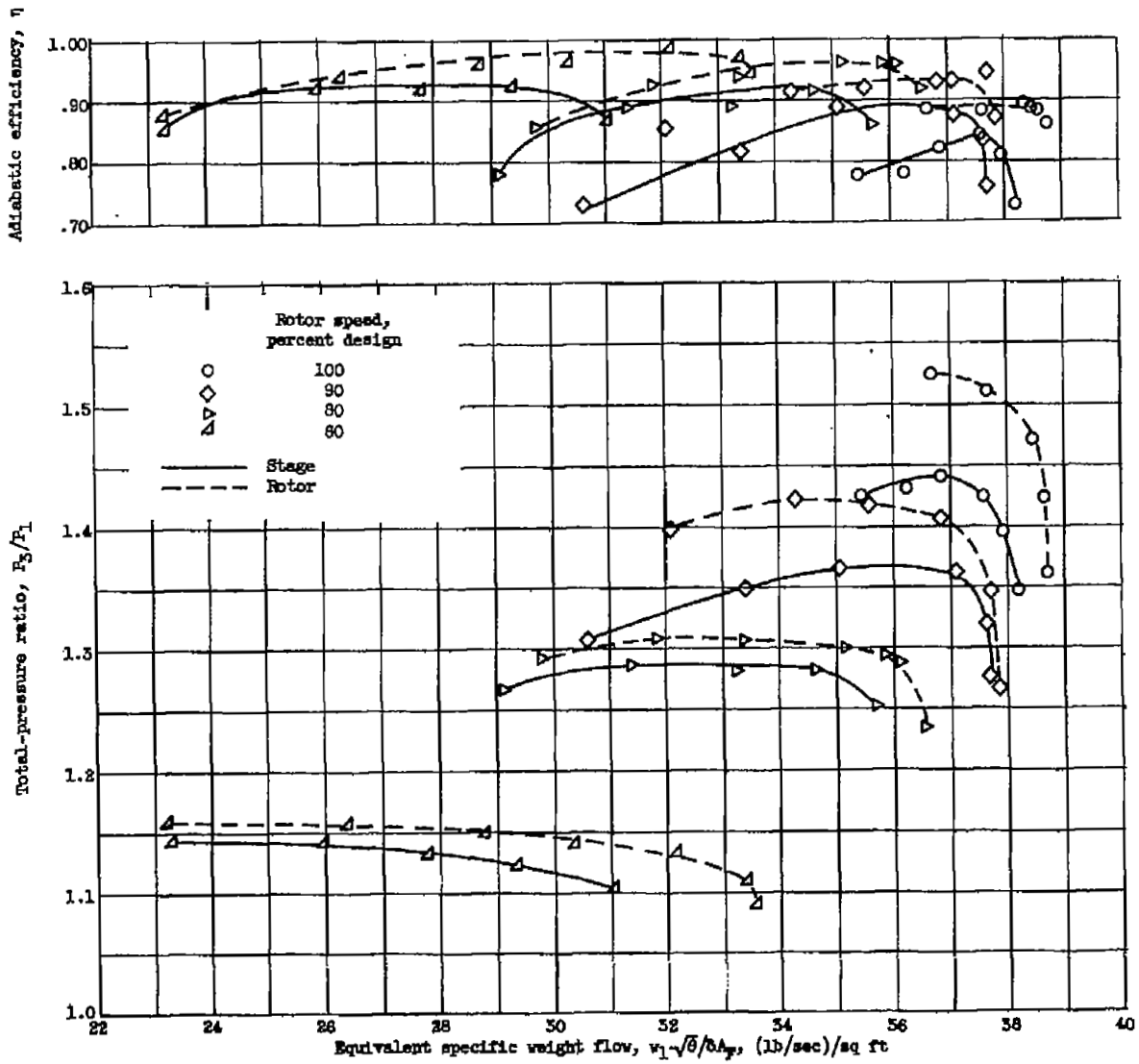

Figure 4. - Mass-averaged over-all performance of 0.55 hub-tip ratio rotor with and without stators.

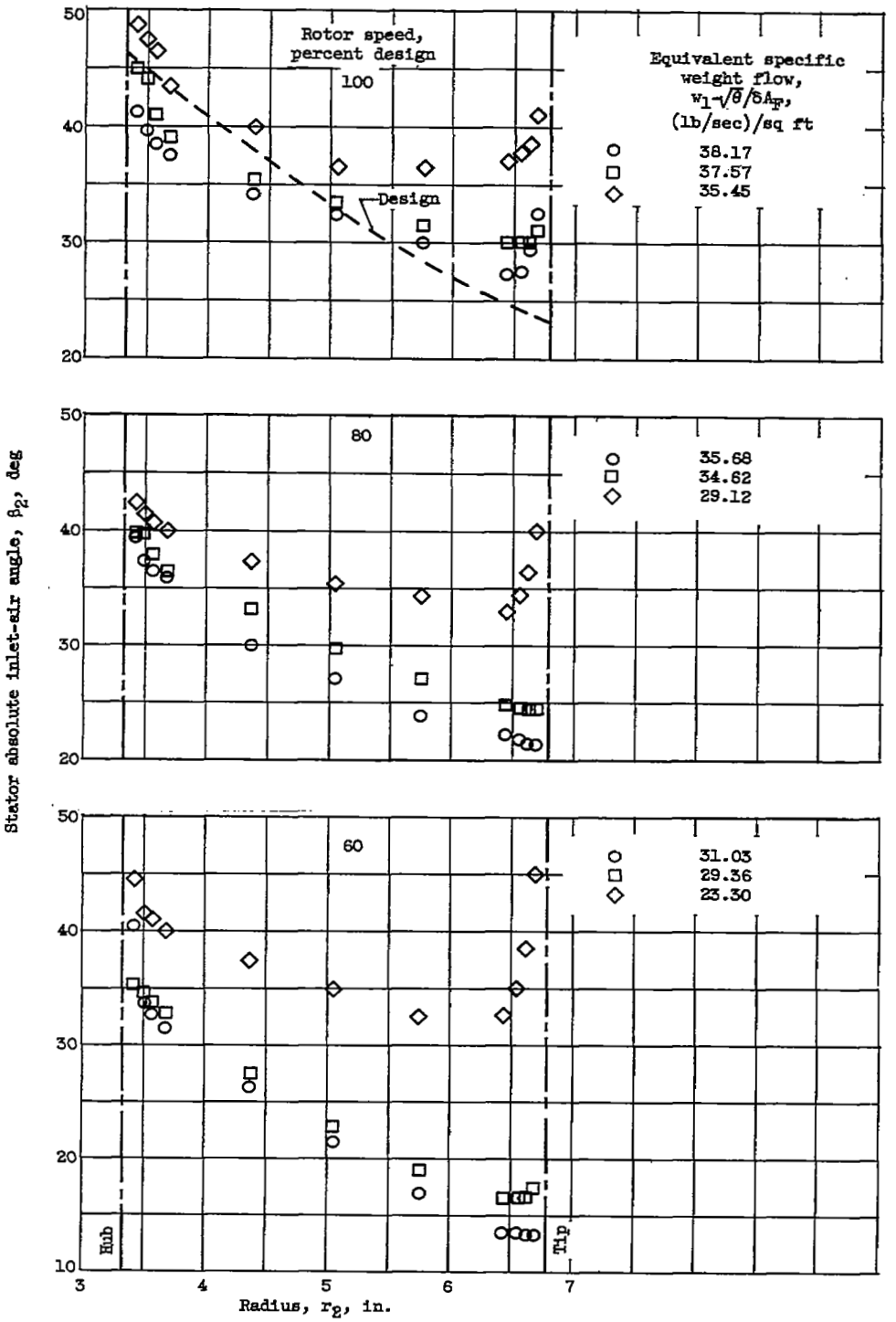

(a) Absolute inlet-air angle.

Figure 5. - Radial variation of stator inlet conditions.

[redacted]

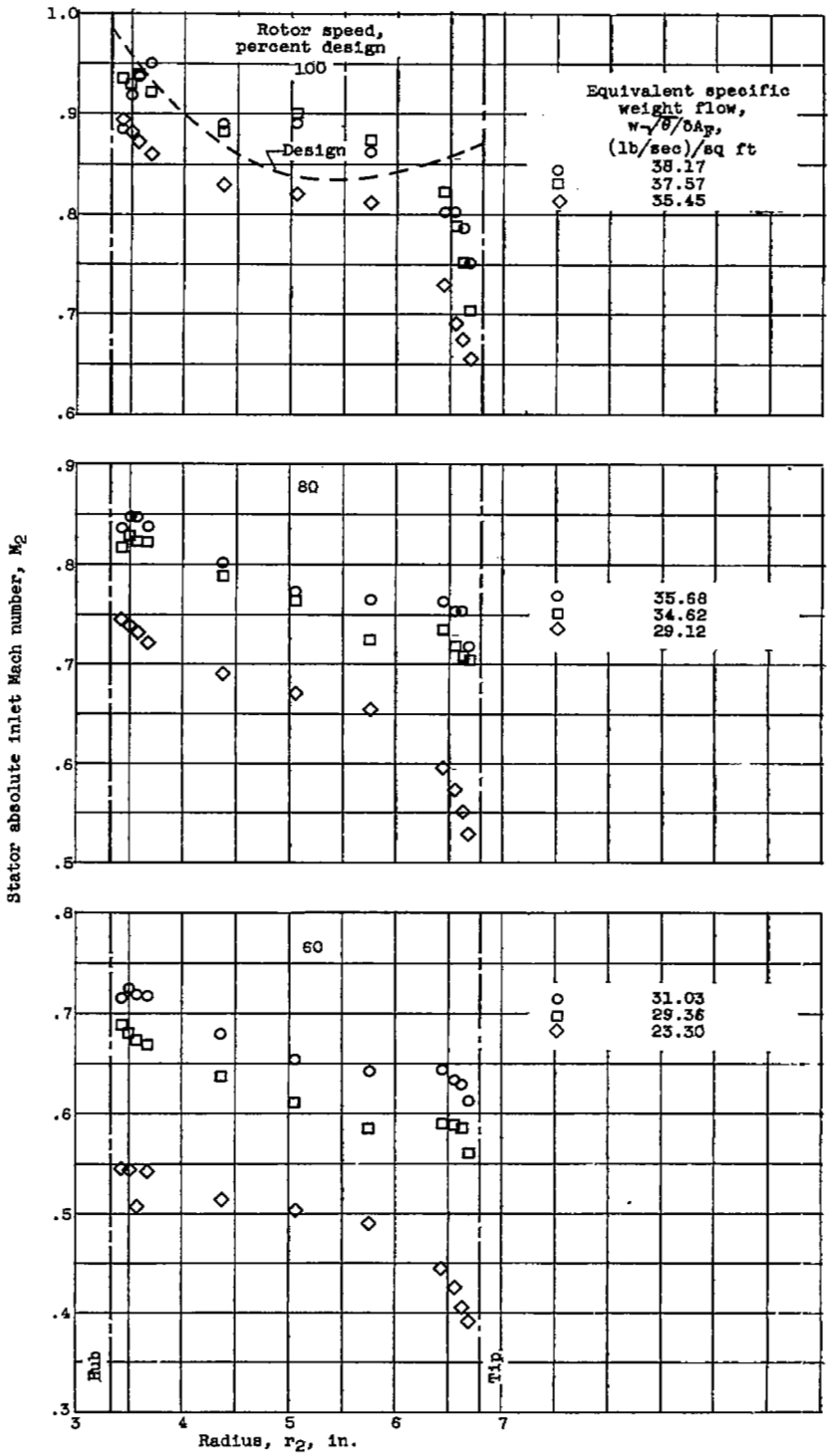

(b) Absolute inlet Mach number.

Figure 5. - Concluded. Radial variation of stator inlet conditions.

[redacted]

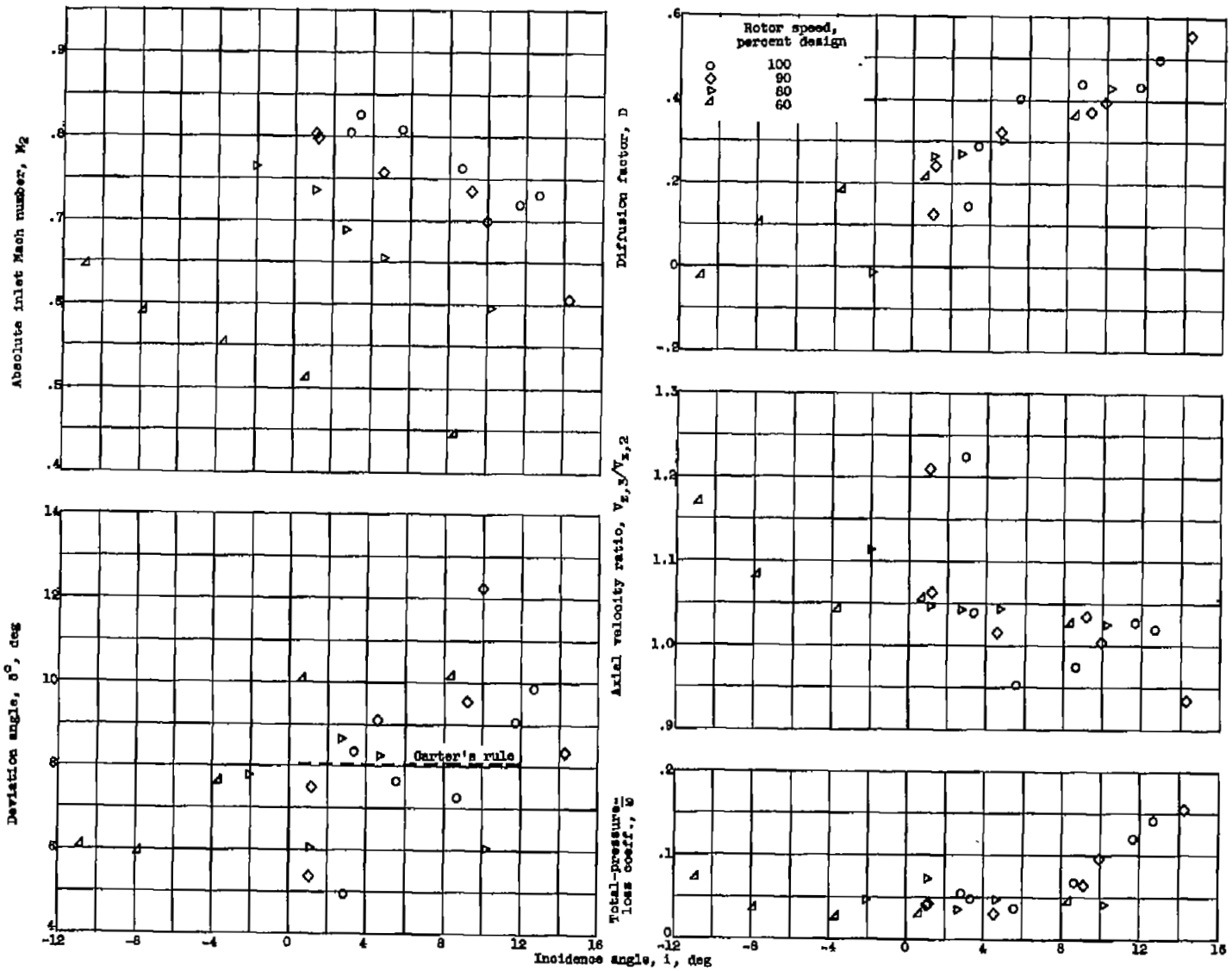

(a) Radial position A: r_3 = 6.48 inches.

Figure 6. - Blade-element performance.

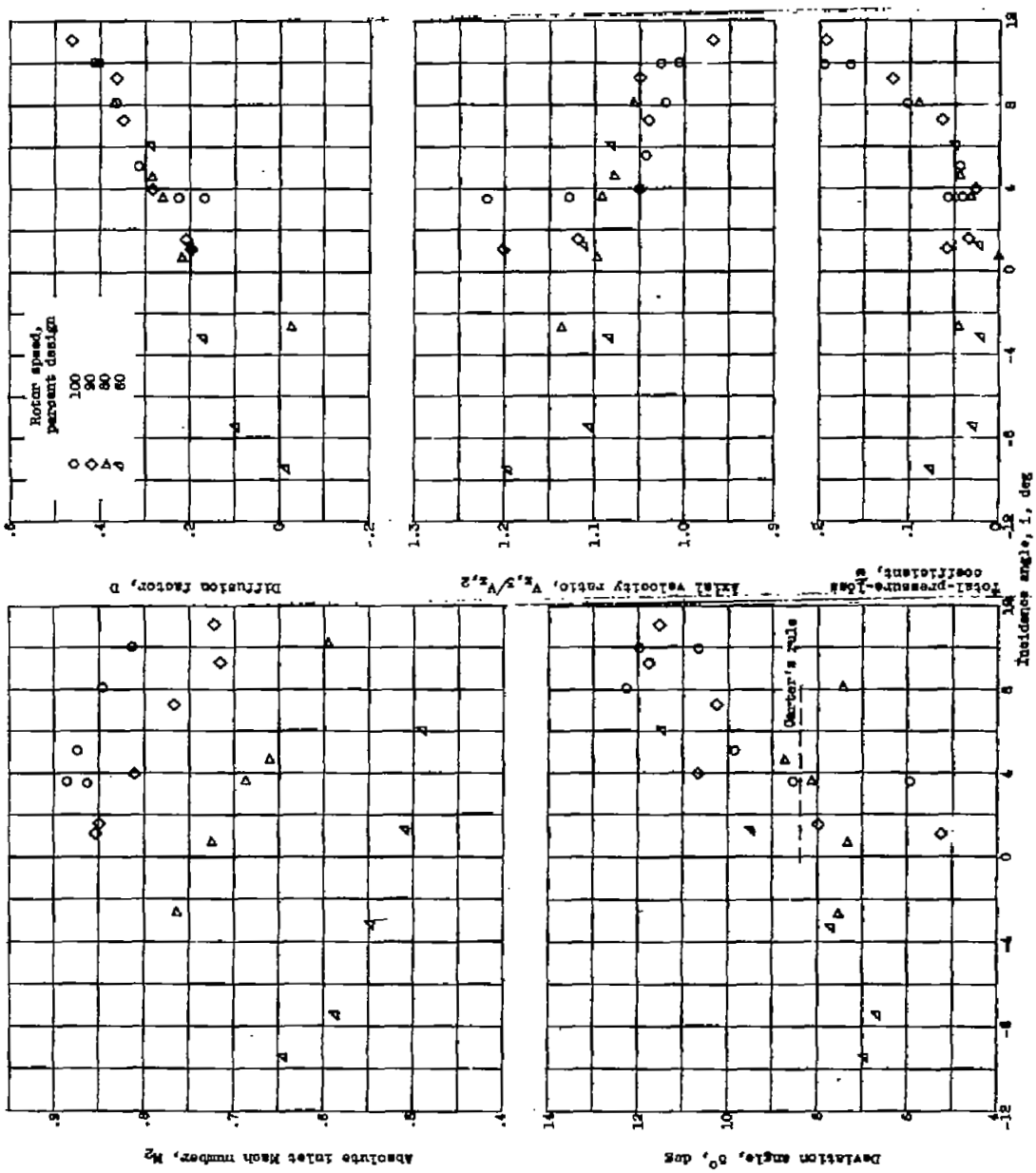

(b) Radial position B: r_3 = 8.67 inches.

Figure 8. - Continued. Blade-element performance.

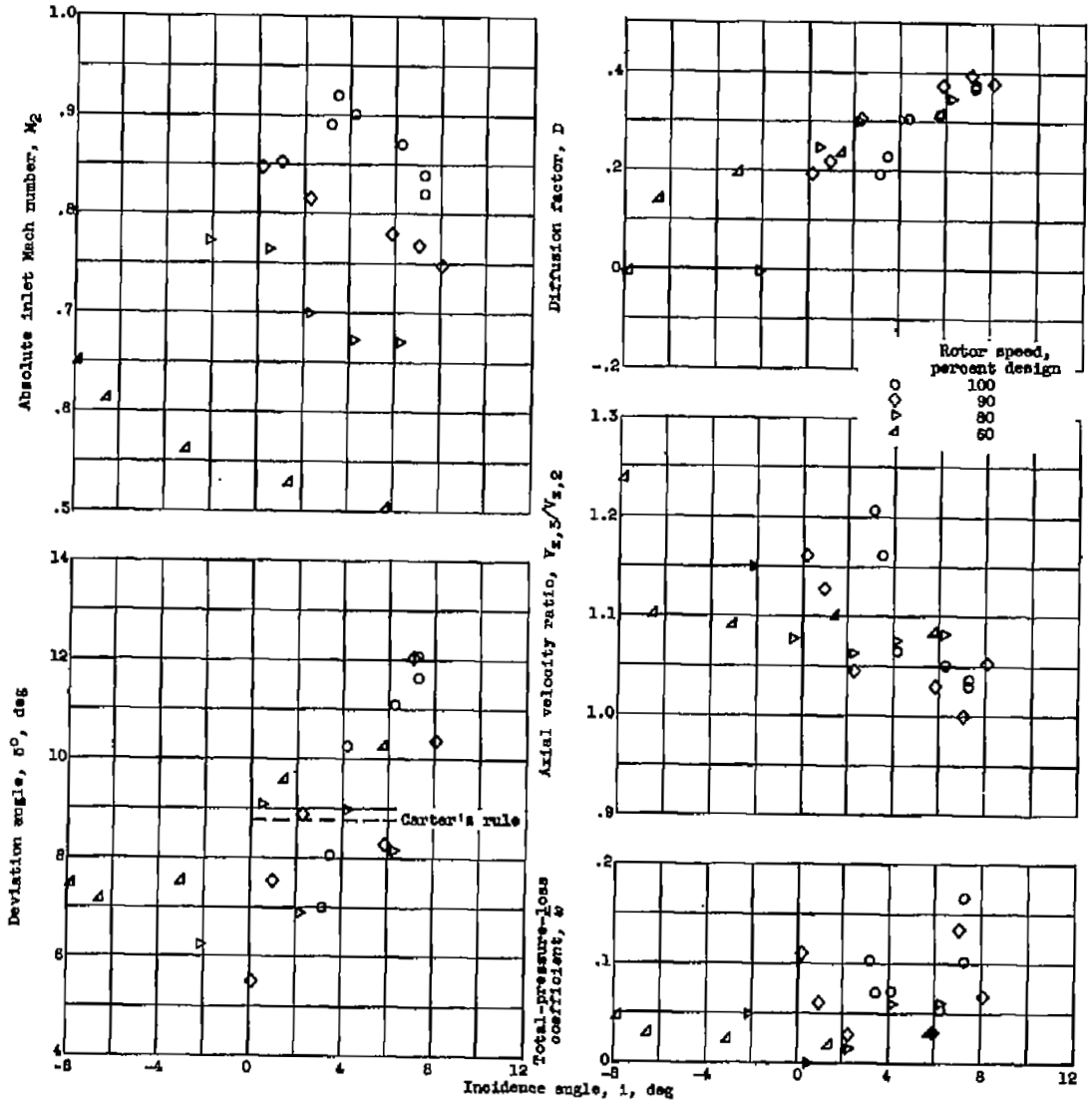

(c) Radial position C: r_2 = 5.28 inches.

Figure 8. - Continued. Blade-element performance.

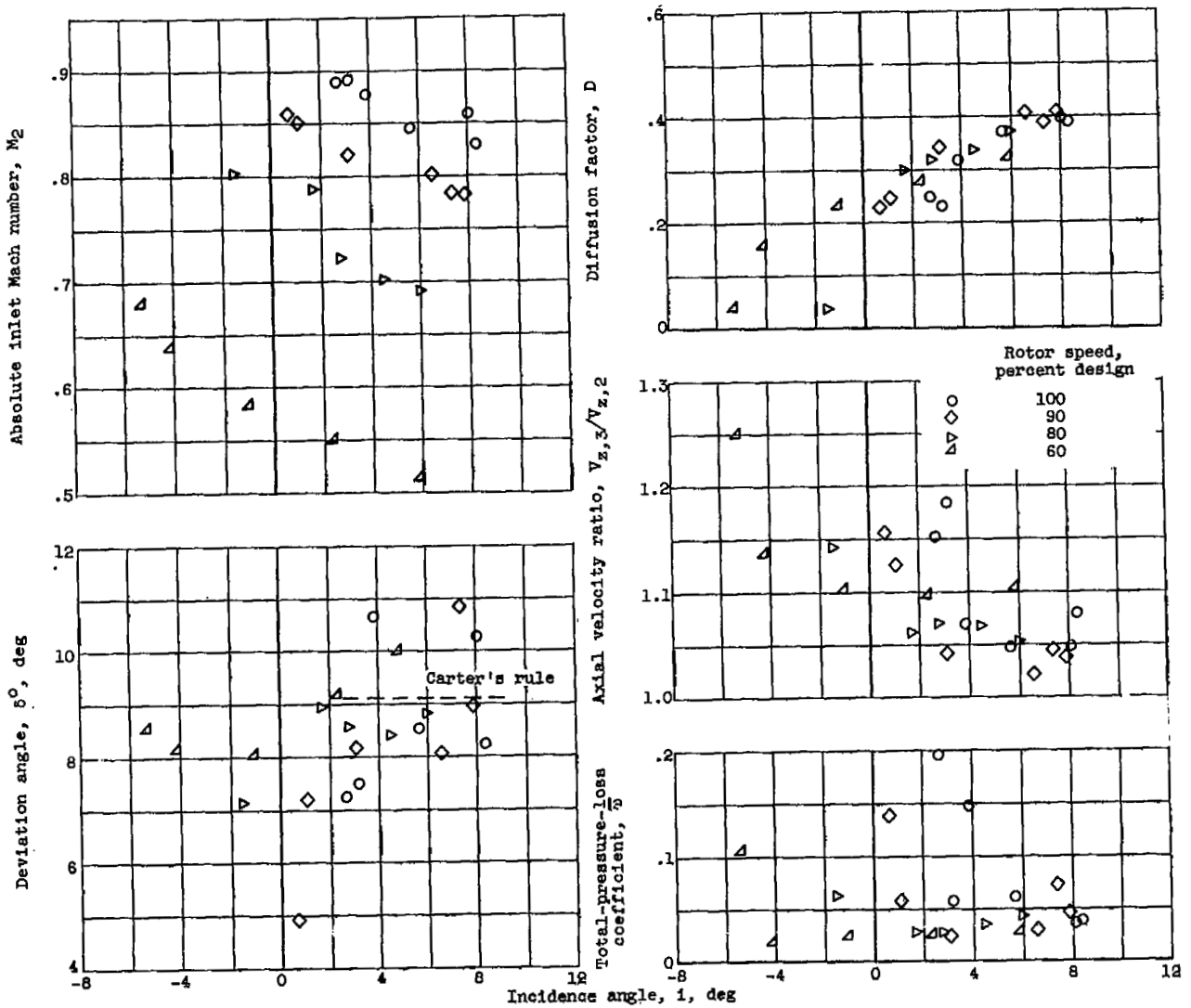

(d) Radial position D: r_3 = 4.64 inches.

Figure 6. - Continued. Blade-element performance.

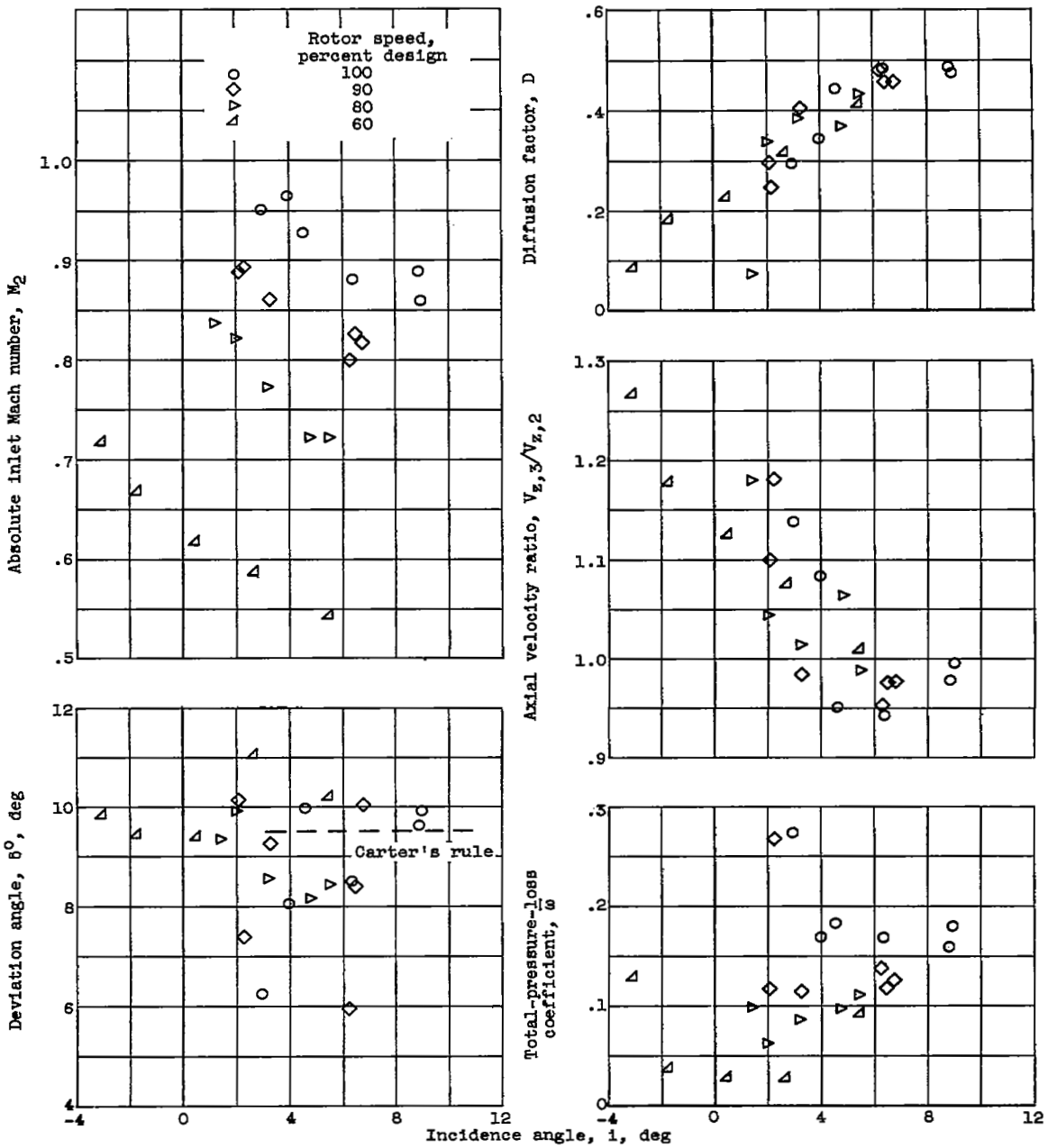

(e) Radial position E: r_3 = 4.03 inches.

Figure 6. - Concluded. Blade-element performance.

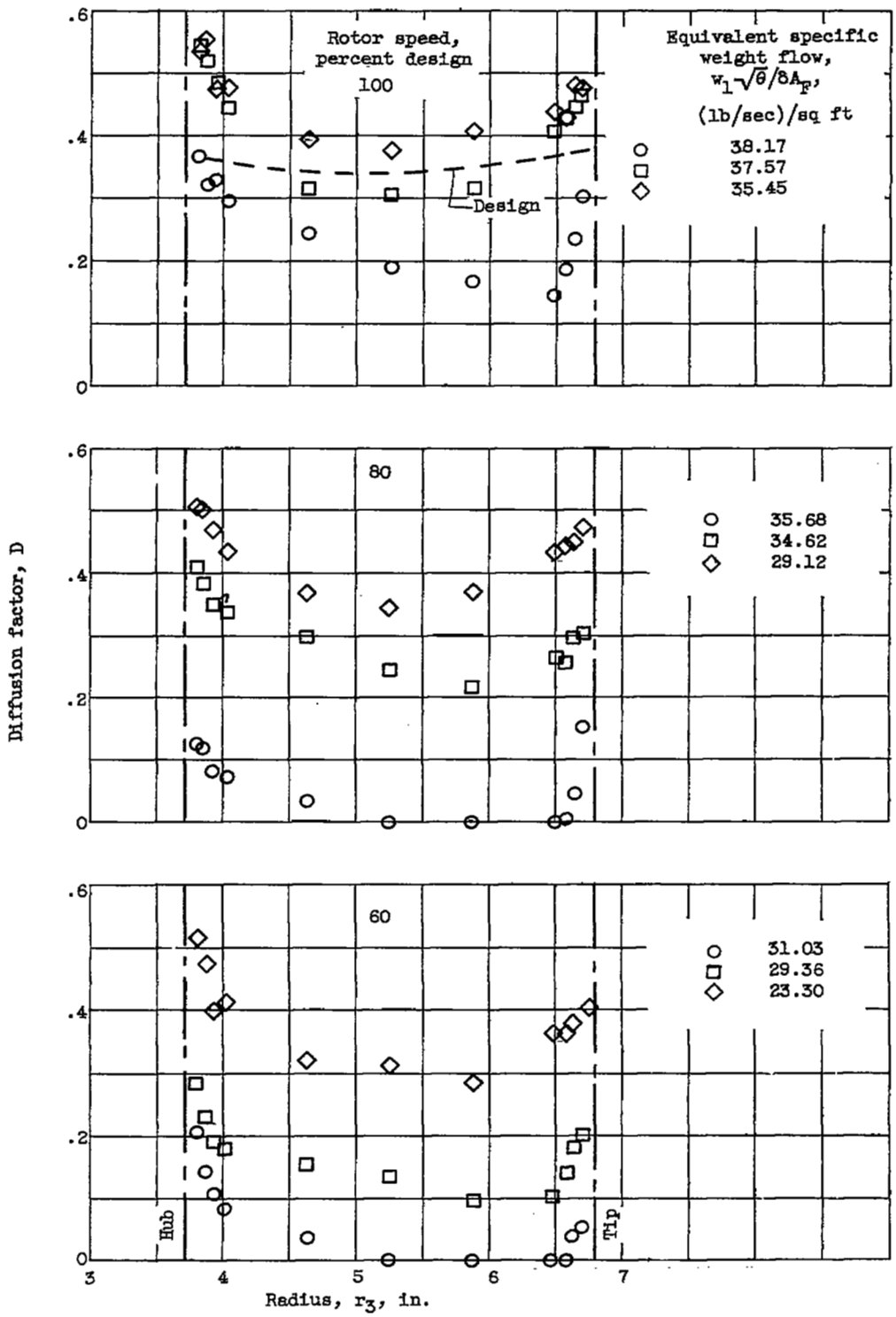

Figure 7. - Radial variation of stator diffusion factor.

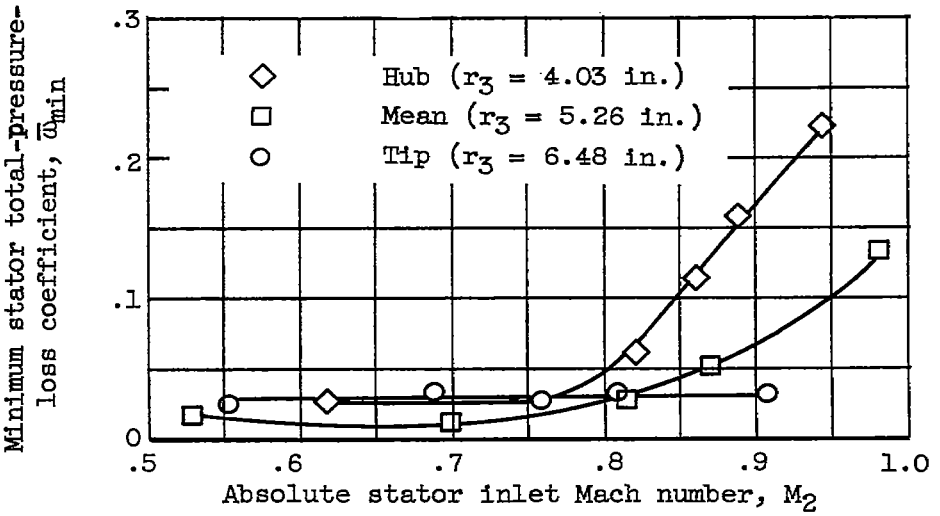

Figure 8. - Variation of stator minimum total-pressure-loss coefficient with absolute inlet Mach number.

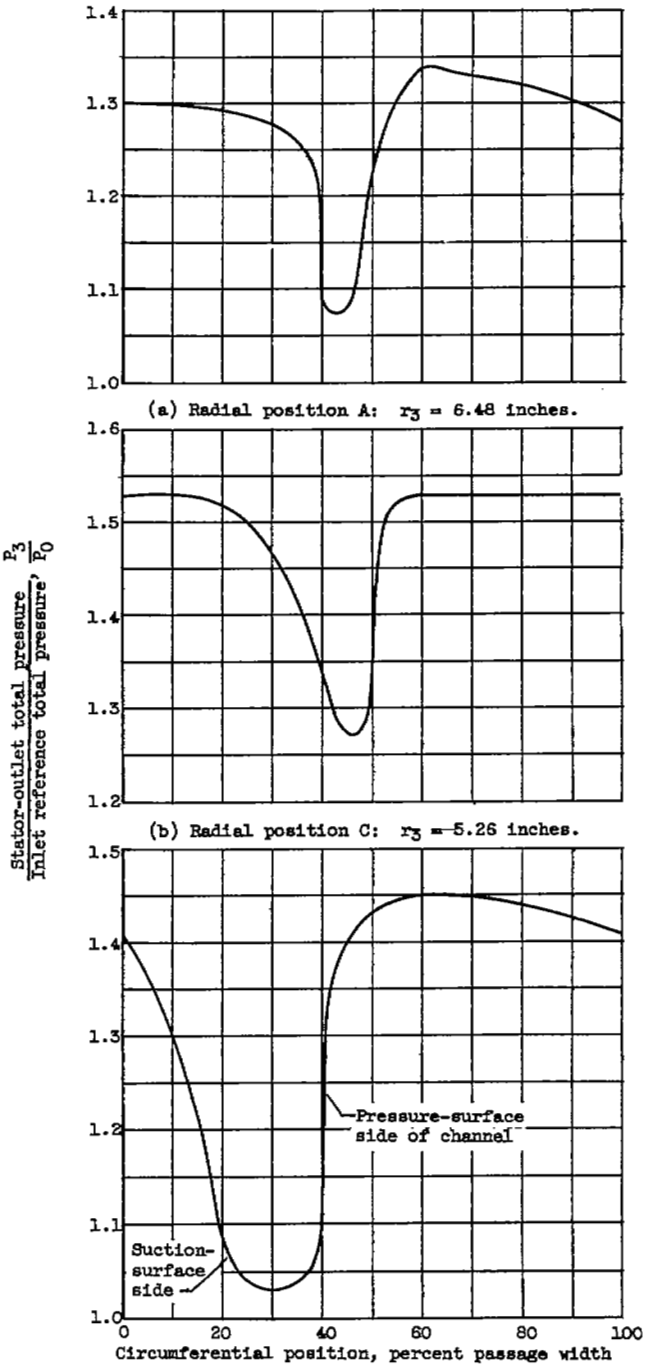

(a) Radial position A: r_3 = 6.48 inches.

(b) Radial position C: r_3 = 5.26 inches.

(c) Radial position E: r_3 = 4.03 inches.

Figure 9. - Circumferential variation of total pressure at stator outlet. Corrected specific weight flow, 37.92 pounds per second per square foot of frontal area at rotor design speed of 1100 feet per second.

[redacted]

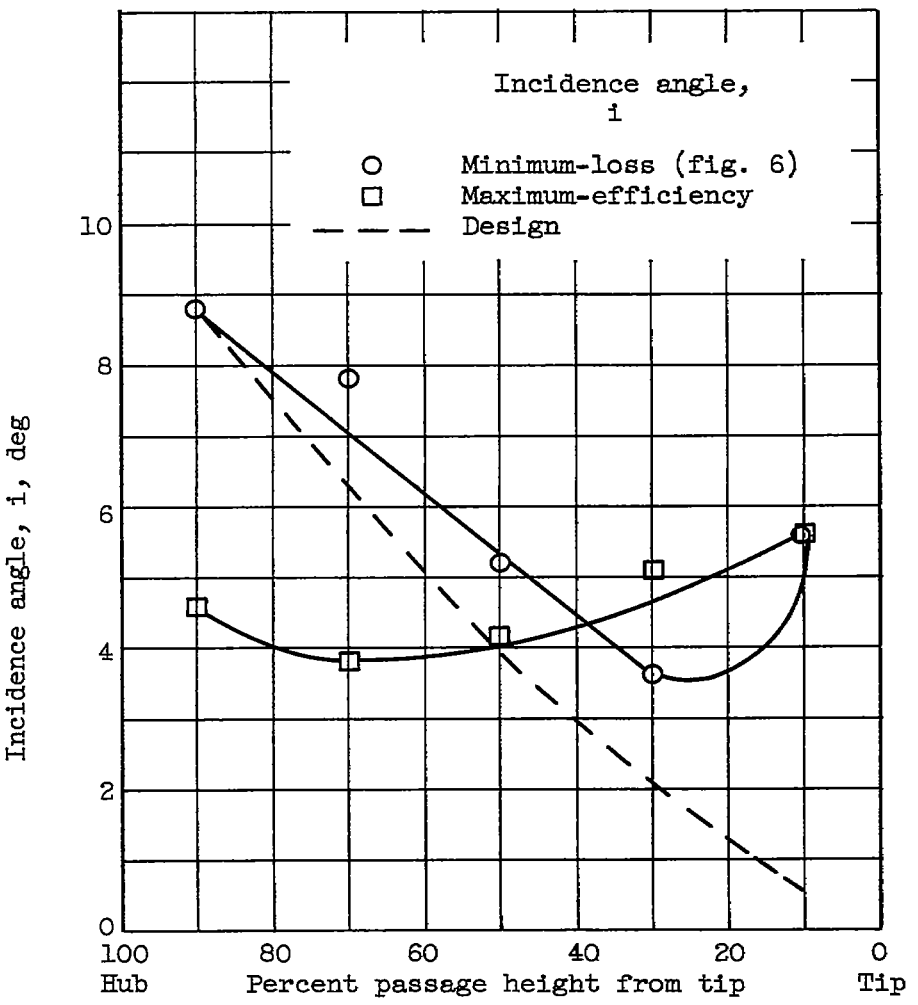

Figure 10. - Incidence-angle variation at design speed.

[redacted]

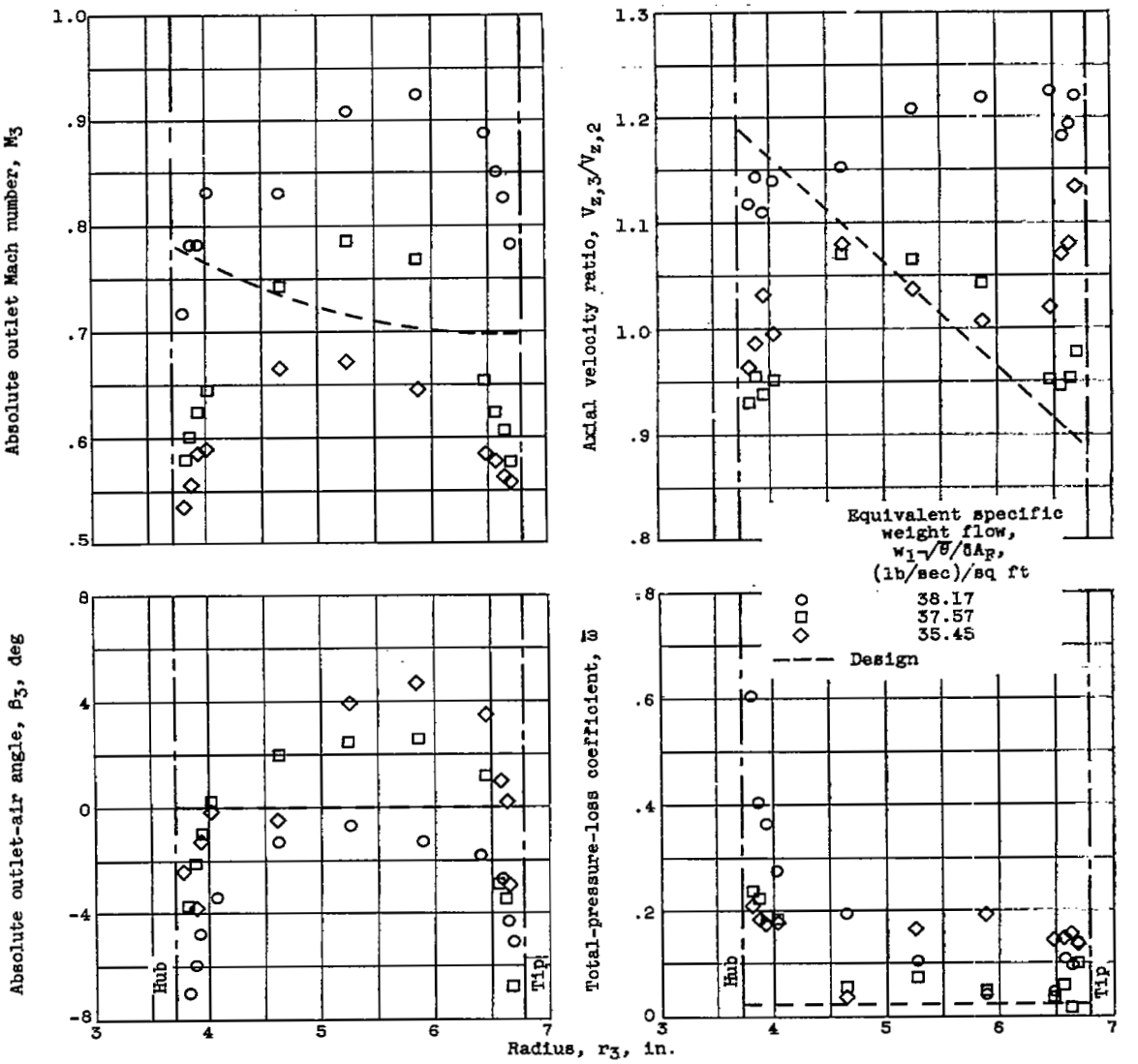

(a) Rotor speed, 100-percent design.

Figure 11. - Radial variation of stator outlet flow parameters.

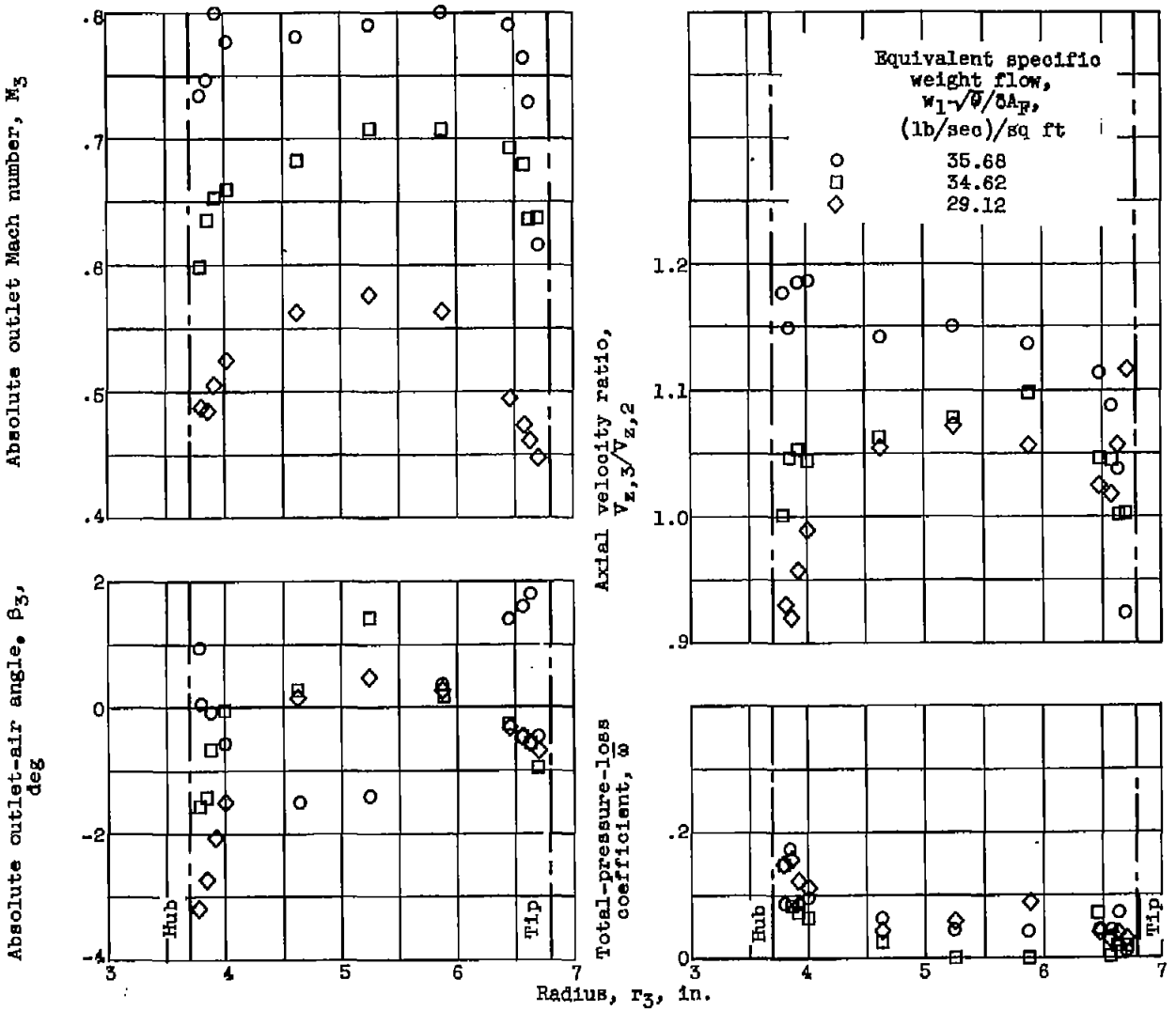

(b) Rotor speed, 80-percent design.

Figure 11. - Continued. Radial variation of stator outlet flow parameters.

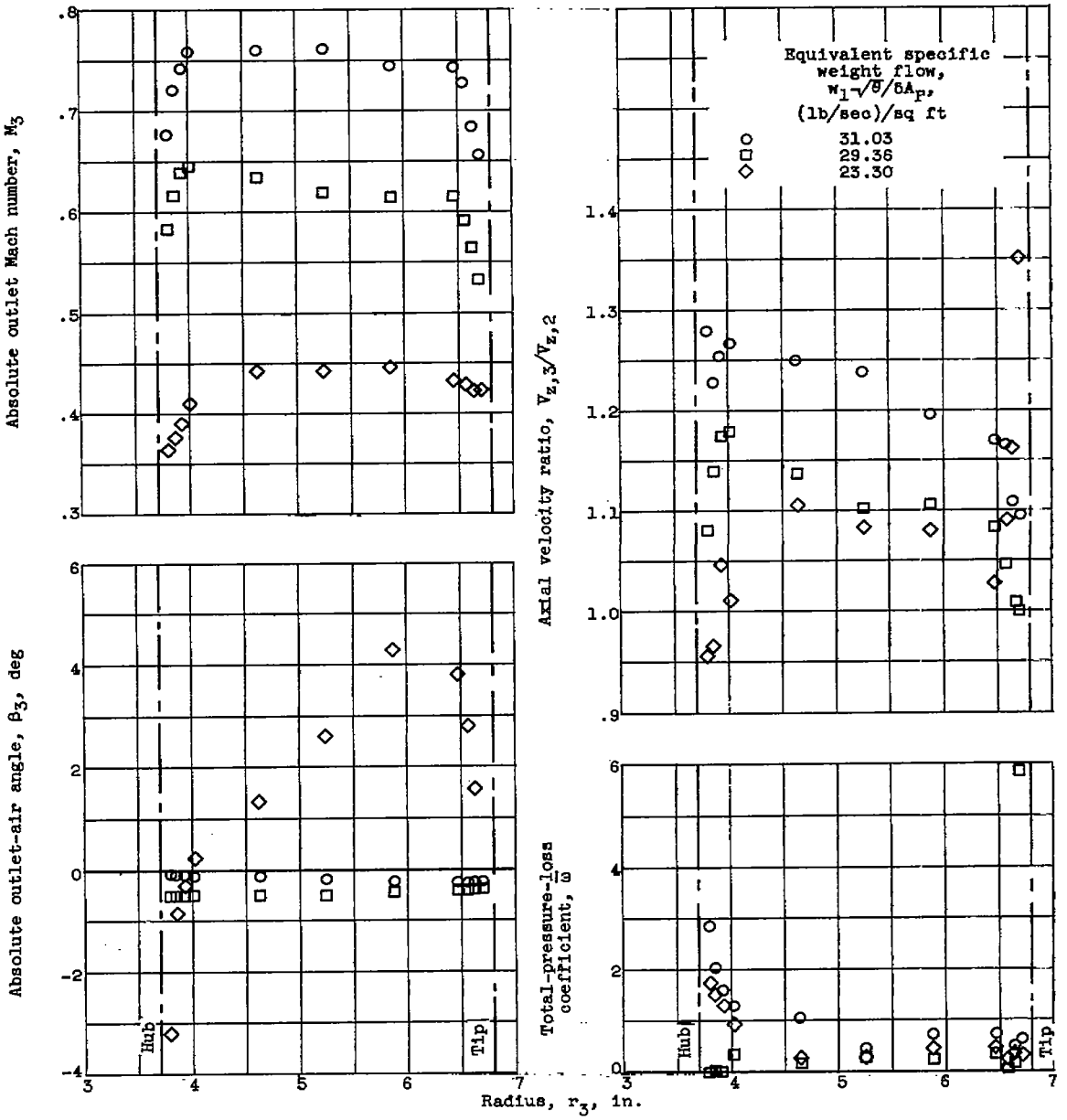

(c) Rotor speed, 60-percent design.

Figure 11. - Concluded. Radial variation of stator outlet flow parameters.